Journal of the Civil Engineering Forum, January 2026, 12(1):40-52
DOI 10.22146/jcef.23135
Available Online at https://jurnal.ugm.ac.id/v3/jcef/issue/archive

Sustainable Concrete Using Ground Granulated Blast Furnace Slag and Polypropylene Fibers: Flexural Behavior of RC Beams

Mardiana Oesman*, Muhamad Irfan Nurdin, Muhammad Miftahul Riza, Wahib Hasan Prasetyo
Department of Civil Engineering, Politeknik Negeri Bandung, Bandung, INDONESIA
*Corresponding author: mardianaoesman@polban.ac.id

SUBMITTED 16 July 2025 **REVISED** 06 September 2025 **ACCEPTED** 23 September 2025

ABSTRACT As sustainability becomes a central focus in the construction industry, the combined use of supplementary cementitious materials and discrete fiber reinforcement offers an innovative pathway to enhance both environmental and structural performance. This study investigates the mechano-microstructural interaction between a dense Ground Granulated Blast Furnace Slag (GGBFS)–based matrix and polypropylene (PP) fibers in reinforced concrete (RC) beams, emphasizing the performance trade-offs among key mechanical properties. The experimental program comprised two phases. First, GGBFS replacement levels of 30% and 45% (by binder mass) were evaluated for compressive strength to identify the optimal matrix. Second, PP fibers were incorporated at 0, 3, 5, and 7 kg/m^3 into the selected matrix. Tests under standardized curing conditions measured compressive strength, flexural load capacity, ductility, toughness, and stiffness. Microstructural analysis assessed fiber–matrix bonding quality and crack-bridging mechanisms. The 30% GGBFS mixture achieved the highest compressive strength in the optimization phase. Fiber inclusion produced distinct performance trade-offs: 3 kg/m^3 delivered the best combination of strength and toughness, 5 kg/m^3 maximized ductility, and 7 kg/m^3 yielded the highest initial stiffness but slightly reduced post-peak energy absorption. These findings demonstrate that no single fiber dosage is universally optimal; instead, the choice should be based on prioritizing specific performance criteria. Microstructural observations revealed dense interfacial transition zones and effective fiber anchorage in GGBFS-rich matrices, enhancing crack control and delaying propagation. This study's primary contribution lies in establishing a clear link between microstructural features and quantified mechanical trade-offs, providing a framework for performance-based mix design. The identified trade-offs also offer direct guidance for performance-based design, enabling engineers to tailor mix compositions to targeted applications such as seismic resilience, deflection-sensitive spans, or impact-resistant members.

KEYWORDS GGBFS; Polypropylene fiber; Reinforced concrete beams; Flexural behavior; Mechano-microstructural interaction; Performance-based design.

1 INTRODUCTION

The mechanical performance of reinforced concrete (RC) beams is fundamentally governed by the synergy between the cementitious matrix and the reinforcement system (Ebead et al., 2017; Qin et al., 2020; Turker and Torun, 2020; Khan et al., 2022; Michalik et al., 2022; Shao et al., 2022; Syll and Kanakubo, 2022; El Mennaouy et al., 2025). When the concrete matrix is densified through supplementary cementitious materials such as Ground Granulated Blast Furnace Slag (GGBFS) fly ash, silica fume, metakaolin, rice husk ash, and when micro- to macro-scale reinforcement is introduced via fibers such as polypropylene (PP), kevlar, carbon, basalt, or steel fibers, an interactive mechanism occurs at both macro and micro levels, (Hawileh et al., 2017; Qin et al., 2019; Hussain et al., 2020; Liu et al., 2021; Prasanna et al., 2021; Ahmad et al., 2022; Lakshmi et al., 2022; Hossain et al., 2022; Xiong et al., 2023; Helmi and Alraimi, 2024; Hendra et al., 2025). The GGBFS enhances matrix compactness through its pozzolanic reaction and latent hydraulic activity, refining pore structure and reducing microvoids (Hawileh et al., 2017; Hussain et al., 2020; Prasanna et al., 2021). Simultaneously, PP fibers act as discrete crack arresters, bridging microcracks and redistributing tensile stresses across the matrix (Qin et al., 2019; Ahmad et al., 2022; Lakshmi et al., 2022).

While previous studies have separately examined the benefits of GGBFS on compressive strength and durability (Özbay et al., 2016; Li, Zhang, Song, Liu and Zhang, 2018; Majhi and Nayak, 2019; Imran et al., 2022), as well as the crack-bridging and toughness-enhancing role of PP fibers (Li et al., 2016; Li, Chi, Xu, Shi and Li, 2018; Gali and Subramaniam, 2019; Hatami Jorbat et al., 2020; Ríos et al., 2020; Bhogone and Subramaniam, 2021; Guo et al., 2021; Liang et al., 2021; Lakshmi et al., 2022; Yan et al., 2024), little is known about their combined mechano-microstructural interaction within a structural element. Specifically, the question remains: how does the microstructural

refinement from GGBFS-based dense matrices interact with the fiber–matrix bonding mechanisms of PP fibers to influence stiffness, ductility, and toughness in RC beams.

This study addresses this gap by designing a two-stage experimental program. In the first stage, different GGBFS replacement levels (30% and 45% by binder mass) were evaluated to identify the mixture with the highest compressive strength. In the second stage, PP fibers were introduced at varying dosages (3, 5, and 7 kg/m³) into the selected GGBFS matrix to investigate their effect on flexural performance. The analysis focuses on quantifying the trade-offs between stiffness, strength, ductility, and toughness, with the aim of developing performance-based design guidance for sustainable, fiber-reinforced concrete in structural applications such as seismic zones, deflection-sensitive spans, and impact-resistant members.

2 METHODS

2.1 Materials Characterization

The cementitious binder consisted of Ordinary Portland Cement (OPC) conforming to ASTM C150 Type I specifications and Ground Granulated Blast Furnace Slag (GGBFS) sourced from a local steel plant. Fine aggregate was natural river sand, and coarse aggregate consisted of crushed stone with a maximum size of 20 mm. PP fibers used in the study had a nominal length of 54 mm, a diameter of approximately 72 µm, a tensile strength of 550 MPa, and a specific gravity of 0.91. Aggregate properties were determined according to Indonesian National Standards (SNI). Cement and GGBFS were evaluated for specific gravity, while reinforcing steel was examined through tensile strength testing to determine yield and ultimate strengths. All material characterization results are presented in Table 1.

2.2 Mix Design and Preparation of GGBFS Concrete

The experimental program consisted of two stages. Stage 1-GGBFS matrix optimization: Two concrete mixtures were prepared with GGBFS replacing Portland cement at 30% and 45% by mass of binder. The total binder content was fixed at 540 kg/m³, and the water-to-binder ratio (*w*/*b*) was maintained at 0.40 for all mixes. A constant superplasticizer dosage of 0.8% by binder mass was used to achieve the target slump. Stage 2- Fiber-reinforced concrete development: The mixture with the higher 28-day compressive strength from Stage 1 was selected as the control matrix for fiber addition. PP fibers were introduced at dosages of 0, 3, 5, and 7 kg/m³. All mixes maintained the same binder composition, aggregate proportions, and admixture dosage as in Stage 1.

2.3 Specimen Preparation and Curing

Concrete was mixed in a pan mixer following ASTM C192. Fibers were gradually added after the aggregates and binder were homogenized, ensuring even distribution and avoiding balling. Cylindrical specimens (100 mm × 200 mm) were cast for compressive strength testing, while RC beams (150 mm × 150 mm × 1000 mm) with steel reinforcement (2Ø10 mm in tension, 2Ø10 mm in compression, stirrups Ø8 mm @ 100 mm) were prepared for flexural testing. All specimens were demolded after 24 hours and water-cured at 23 ± 2 °C until the designated testing ages.

2.4 Testing Procedures

Workability was assessed using the flow table test for Stage 1 mixtures, and the slump test for Stage 2 mixtures. Compressive strength tests were conducted at 7, 28, and 56 days following SNI 03-1974-2011, with three specimens tested for each age and mix, and the mean values reported. Flexural performance was evaluated at 56 days using a four-point bending test in accordance with ASTM C78. Load–deflection behavior was recorded with a linear variable displacement transducer (LVDT) positioned at mid-span. The parameters measured included peak load (P_{max}), ultimate load (P_{ult}, defined as 80% of P_{max} on the descending branch), initial stiffness (slope of the initial linear portion of the load–deflection curve), ductility index (ratio of ultimate deflection to yield deflection, as suggested by Ling et al. (2023)), and toughness (area under the load–deflection curve until failure). Crack patterns were photographed at both P_{max} and P_{ult}, crack width and distribution were qualitatively analyzed to relate cracking behavior to mechanical performance.

3 RESULTS

3.1 Compressive Strength of Concrete with GGBFS and PP Fibers

Compressive strength tests were conducted at curing ages of 7, 28, and 56 days to examine the influence of GGBFS replacement on strength development. The results are presented in Table 2 and Figure 1. The mixture containing 30% GGBFS achieved the highest compressive strength at 28 days (29.42 MPa) and continued to gain strength up to 56 days (30.64 MPa). In comparison, the 45% GGBFS mixture exhibited lower strength at both ages, while the control mix without GGBFS showed the highest early strength but a less pronounced gain after 28 days.

At the early age of 7 days, the control mixture recorded 31.31 MPa, significantly higher than both slag-containing mixes, which registered 14.17 MPa

Table 1. Results of material characterization tests

Material / Test Type	Test Standard	Result
Cement		
Specific gravity	SNI 2531:2015	2.93 g/cm^3
Ground Granulated Blast Furnace Slag (GGBFS)		
Specific gravity	SNI 2531:2015	2.84 g/cm^3
Coarse Aggregate		
Compacted unit weight	SNI 03-4804:1998	1.50 g/cm^3
Loose unit weight	SNI 03-4804:1998	1.41 g/cm^3
Saturated surface-dry (SSD) specific gravity	SNI 1970:2016	2.59
Bulk specific gravity (SSD)	SNI 1970:2016	2.50
Apparent specific gravity	SNI 1970:2016	2.74
Water absorption	SNI 1970:2016	3.42%
Passing sieve No. 200	SNI 03-4142:1996	1.39%
Fine Aggregate		
Compacted unit weight	SNI 03-4804:1998	1.77 g/cm^3
Loose unit weight	SNI 03-4804:1998	1.72 g/cm^3
Saturated surface-dry (SSD) specific gravity	SNI 1970:2016	2.54
Bulk specific gravity (SSD)	SNI 1970:2016	2.45
Apparent specific gravity	SNI 1970:2016	2.70
Water absorption	SNI 1970:2016	3.81%
Passing sieve No. 200	SNI 03-4142:1996	5.87%
Organic matter content	SNI 2816:2014	Number 1
Reinforcing Steel		
Yield strength (f_y)	SNI 2052:2017	375.95 MPa
Ultimate tensile strength (f_u)	SNI 2052:2017	526.34 MPa

(30% GGBFS) and 15.27 MPa (45% GGBFS). This result reflects the well-established phenomenon that GGBFS replacement reduces early-age strength due to the slower kinetics of the pozzolanic and latent hydraulic reactions compared to the rapid hydration of Portland cement clinker minerals. While this early reduction in strength may be a concern for applications requiring rapid formwork removal or early loading, it is important to note that such limitations can be mitigated through adjustments in the curing regime or supplementary acceleration methods.

Table 2. Compressive strength development over time for varying GGBFS replacement levels

GGBFS variations	7 day (MPa)	28 day (MPa)	56 day (MPa)
Control	31.31	23.09	26.37
30% GGBFS	14.17	29.42	30.64
45% GGBFS	15.27	21.34	27.45

Between 7 and 28 days, a notable strength gain was observed in the 30% GGBFS mixture, surpassing the control mixture at 28 days. The continuous availability of calcium hydroxide from cement hydration promotes ongoing secondary reactions with GGBFS, leading to the formation of additional calcium silicate hydrate (C–S–H) gel. This additional C–S–H fills microvoids within the paste, thereby refining the pore structure and improving the density of the hardened matrix. The slower yet prolonged hydration of GGBFS is advantageous for long-term structural performance, as it contributes to higher later-age strengths, reduced permeability, and improved durability.

By 56 days, all mixtures exhibited further strength development, though the relative gains varied. The control mixture improved modestly to 26.37 MPa, while the 30% GGBFS mix reached 30.64 MPa, maintaining its superior performance. The 45% GGBFS mixture also improved to 27.45 MPa but remained lower than the 30% mix. This confirms that excessive GGBFS content can lead to dilution of clinker phases and insufficient calcium hydroxide for complete activation of the slag

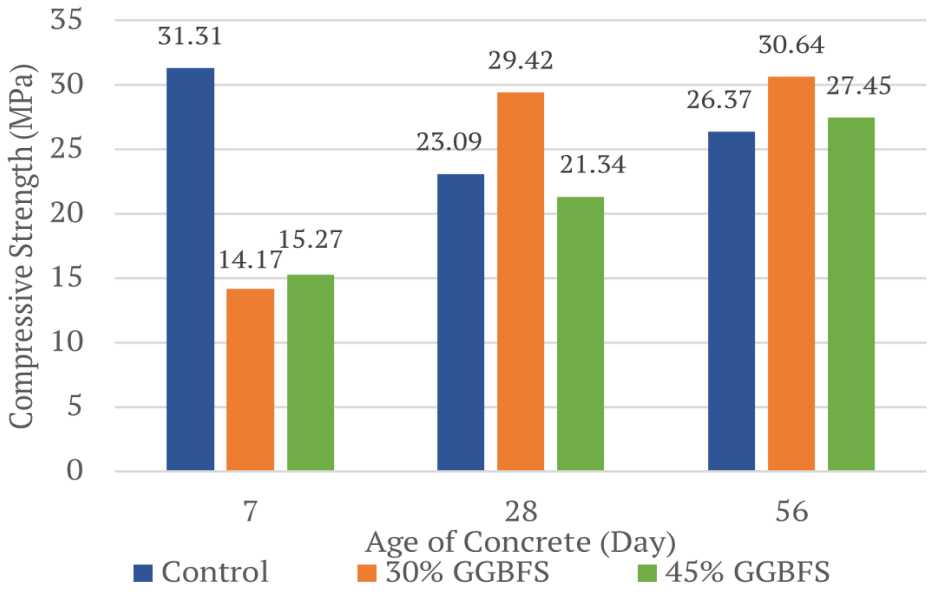

Figure 1 Compressive strength development over time for concrete mixtures with varying GGBFS replacement levels (0%, 30%, 45%) at 7, 28, and 56 days.

particles, resulting in a plateau or reduction in later-age strength. This finding is consistent with Oner and Akyuz (2007), who reported optimal GGBFS replacement levels between 30% and 40% for achieving the best balance between early and later-age strength.

From a structural engineering perspective, the implications of these results are significant. For applications where long-term load-carrying capacity, low permeability, and high durability are prioritized—such as bridge decks, marine structures, and high-rise building columns—using 30% GGBFS provides an optimal balance between strength development and sustainability benefits. Additionally, the reduced early-age strength of GGBFS concrete can be advantageous in massive pours, as the slower heat evolution lowers the risk of thermal cracking.

Comparing these findings with the review by Muralidharan et al. (2021) on supplementary cementitious materials, the strength development pattern observed here aligns with the general behavior of slag-blended systems, which typically underperform at early ages but outperform plain cement mixes at later ages, especially beyond 56 or 90 days. This suggests that even higher long-term strength gains could be expected if testing were extended to 90 days or one year.

In summary, the 30% GGBFS mixture demonstrated the most favorable strength development profile, balancing initial strength reduction with substantial later-age gains. This performance, combined with its environmental benefits through reduced cement content, supports its suitability for sustainable structural concrete design.

3.2 Effect of PP Fibers on Compressive Strength

The influence of polypropylene (PP) fiber content on the compressive strength of concrete with a 30% GGBFS matrix was evaluated at 28 and 56 days. The results, summarized in Table 3 and Figure 2, indicate that fiber addition had a measurable effect on both early and later-age compressive strength.

At 28 days, the control mix without fibers (PP0) achieved 24.13 MPa, whereas all fiber-reinforced mixtures showed significantly higher strengths. The PP3 mixture (3 kg/m^3 fiber) reached the highest value at 34.73 MPa, representing a 43.9% improvement over the control. The PP5 and PP7 mixtures recorded slightly lower strengths of 34.40 MPa and 34.28 MPa, respectively. This trend suggests that moderate fiber content enhances compressive strength, but additional fibers beyond an optimal dosage yield diminishing returns.

At 56 days, a similar pattern was observed. The control mix improved to 37.66 MPa, narrowing the gap with the fiber-reinforced mixes. Nevertheless, PP3 maintained the highest strength (39.49 MPa), followed closely by

Table 3. Compressive strength of concrete specimens incorporating varying PP fiber contents

PP fiber variations	28 day (MPa)	56 day (MPa)
0 kg/m^3	24.13	37.66
3 kg/m^3	34.73	39.49
5 kg/m^3	34.40	38.22
7 kg/m^3	34.28	38.06

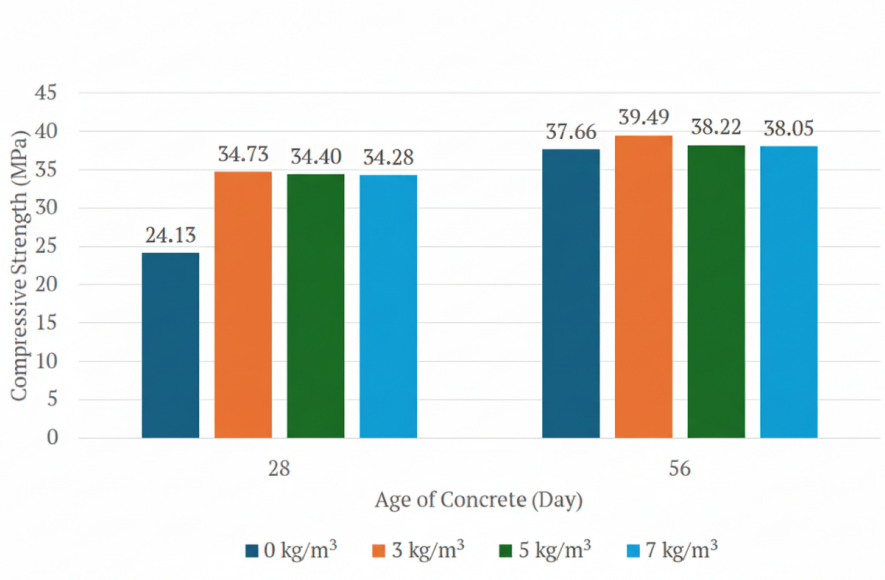

Figure 2 Compressive strength at 28 and 56 days for concrete mixtures with varying PP fiber contents (0, 3, 5, 7 kg/m³) in the selected 30% GGBFS matrix.

PP5 (38.22 MPa) and PP7 (38.06 MPa). The sustained advantage of PP3 at later ages suggests that an optimal fiber dosage not only bridges microcracks but also integrates effectively within the dense GGBFS matrix, maintaining good fiber–matrix bonding and reducing stress concentrations under load.

The improvement in compressive strength at moderate fiber content can be explained by several mechanisms. First, the presence of PP fibers helps to arrest microcrack formation during early shrinkage and under service loads, thereby preserving the integrity of the cement paste before significant damage develops. Second, in a dense GGBFS matrix, the interfacial transition zone (ITZ) between fibers and paste is enhanced due to the refined pore structure, leading to better stress transfer. Third, fibers may contribute to load sharing within the composite during compression, particularly when cracks initiate, by restraining crack opening and redistributing stresses.

However, at higher dosages (5–7 kg/m³), the slight reduction in strength is likely due to fiber balling and reduced workability, which can introduce entrapped air and localized weak zones. This effect has been reported in prior studies, such as (Banthia and Gupta, 2006; Bertelsen et al., 2020), which noted that excessive fiber volume can disrupt paste continuity and lead to compaction difficulties, particularly in mixes with a lower water-to-binder ratio. In the present study, this phenomenon was more pronounced given the already low *w/b* ratio and dense matrix provided by GGBFS, which leaves little tolerance for workability loss without mechanical vibration adjustments.

From a practical standpoint, these results suggest that incorporating 3 kg/m³ of PP fibers into a 30% GGBFS concrete matrix provides an optimal balance between compressive strength enhancement and workability. For structural applications where compressive strength is a primary performance requirement—such as columns, prestressed beams, or heavily loaded slab elements—this dosage offers tangible benefits without introducing mixing or placement challenges.

It is also important to note that while compressive strength is a critical property, it is not the sole determinant of structural performance, particularly in fiber-reinforced systems. The full benefit of PP fibers emerges in post-cracking behavior, ductility, and energy absorption, which will be discussed in the subsequent flexural performance sections. Nevertheless, establishing that fiber inclusion at optimal levels does not compromise, and can even enhance, compressive strength is essential for validating the viability of such composites in practical structural applications.

In summary, the experimental findings confirm that moderate PP fiber content (around 3 kg/m³) enhances compressive strength in a dense GGBFS matrix, while higher contents may slightly reduce strength due to workability issues. These observations align with existing literature and reinforce the need for careful optimization of fiber dosage in performance-based concrete mix design.

3.3 Flexural Behavior of RC Beams

The flexural performance of RC beams incorporating 30% GGBFS with varying PP fiber dosages (0, 3, 5, and 7 kg/m³) was evaluated through four-point bending tests at 56 days. The load–deflection curves (Figure 3) demonstrated that all beams exhibited an initial

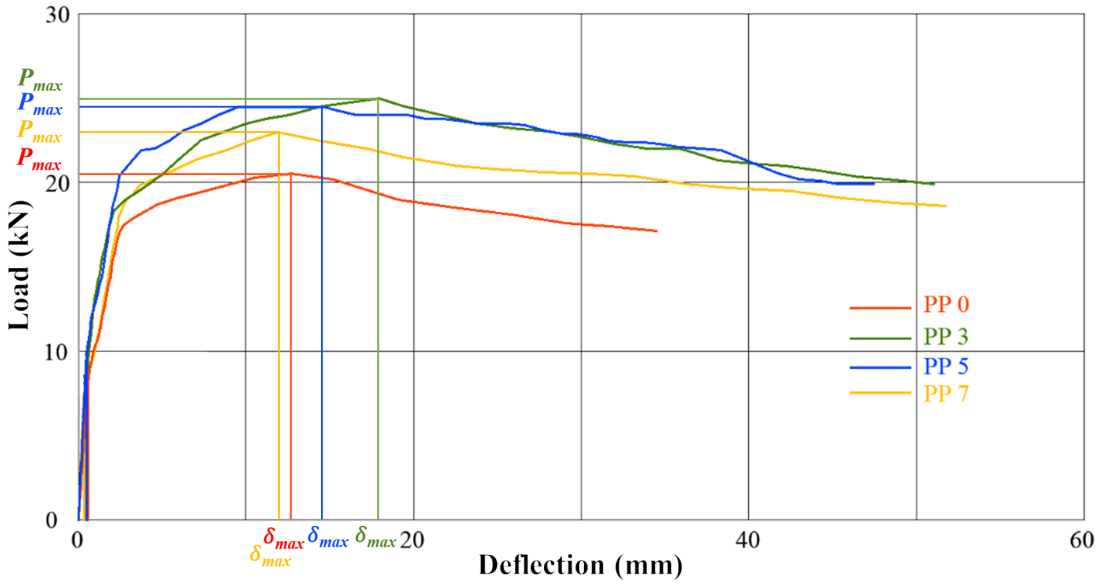

Figure 3 Load–deflection curves of RC beams with 30% GGBFS matrix and varying PP fiber contents (0, 3, 5, 7 kg/m³), showing P_{max} and P_{ult} points.

linear elastic response followed by nonlinear behavior until failure. The inclusion of PP fibers enhanced both peak load (P_{max}) and post-cracking performance compared to the control beam (PP0).

As shown in Table 4, the highest maximum load was achieved with PP3 (25.0 kN), representing a 21.95% increase over the control beam's 20.5 kN. This improvement indicates that a moderate fiber dosage effectively contributes to crack-bridging and stress redistribution, allowing better utilization of the tensile reinforcement before peak load is reached. The PP5 and PP7 beams recorded slightly lower P_{max} values (24.5 and 23.0 kN, respectively) compared to PP3, suggesting that excessive fiber content may reduce workability and lead to uneven fiber distribution ("balling"), which in turn impairs matrix homogeneity and load transfer efficiency.

Deflection at maximum load also increased with fiber inclusion, most notably for PP3 (17.94 mm) compared to PP0 (12.71 mm). This result reflects enhanced strain capacity before peak loading, indicating that fibers help delay crack localization. However, in the PP7 beam, despite a higher fiber content, the deflection at P_{max} was lower (11.88 mm) than that of PP3 and PP5, suggesting that excessive stiffness at high fiber dosages can limit elastic deformation capacity.

When considering post-peak behavior, all fiber-reinforced beams displayed a more gradual load reduction compared to the brittle drop observed in the control beam. The ultimate deflection (δ_{ult}) was highest in PP7 (51.74 mm), followed closely by PP3 (51.00 mm) and PP5 (47.41 mm), while the control beam reached only 34.80 mm. This demonstrates that fiber inclusion significantly enhances the deformation capacity of beams beyond peak load, enabling them to sustain greater deflections before failure.

The ductility index, defined as the ratio of δ_{ult} to δ_{yield}, reached its maximum in PP5 (14.41), which was 43.38% higher than the control. The superior ductility at this dosage may be attributed to an optimal combination of fiber dispersion and matrix–fiber bond strength, which provides effective crack control without inducing the stiffness-related limitations observed in PP7. Higher ductility is particularly beneficial in seismic design, as it allows the structure to absorb and dissipate energy over a longer deformation range.

Initial stiffness, calculated from the slope of the initial linear portion of the load–deflection curve, increased consistently with fiber content: from 14.27 kN/mm in PP0 to 24.10 kN/mm in PP7. This stiffening effect can be attributed to the improved integrity of the matrix, where GGBFS-induced densification reduces microvoids, and fibers restrain incipient microcracks, thus delaying the onset of nonlinear deformation. However, while high stiffness improves serviceability by reducing deflections under working loads, overly stiff beams (such as PP7) may experience reduced post-cracking deformability, which could be undesirable in applications requiring high ductility.

Energy absorption (area under the load–deflection curve up to P_{max}) was highest for PP3 (379.66 kN·mm), an increase of 68% over the control. This indicates that PP3 achieves the most efficient fiber–matrix interaction in the elastic and early post-cracking phases. Energy dissipation (area beyond P_{max} until failure) continued to increase with fiber content, peaking in PP7 (814.11 kN·mm). The higher dissipation in PP7 sug-

Table 4. Recapitulation of flexural performance of FRC beams

Behavior	PP0	PP3	PP5	PP7
Max Load ($P_{\max}$, kN)	20.50	25.00	24.50	23.00
Deflection $P_{\max}$ (mm)	12.71	17.94	14.68	11.88
Ultimate Load (kN)	17.10	19.90	19.90	18.60
Deflection P_{ult} (mm)	34.80	51.00	47.41	51.74
Initial Stiffness (kN/mm)	14.27	18.10	21.70	24.10
Ductility Index	10.05	11.59	14.41	13.83
Yield Load (kN)	17.96	20.48	21.20	19.95
Deflection Yield (mm)	3.43	4.40	3.29	3.95
Energy Absorption (kN·mm)	225.37	379.66	320.02	227.79
Energy Dissipation (kN·mm)	403.5	717.65	734.44	814.11
Toughness (kN·mm)	628.87	1097.31	1054.46	1041.90

gests that although peak load capacity is slightly lower, the beam can release stored elastic energy more gradually, reducing the risk of sudden brittle failure. The overall toughness (sum of energy absorption and dissipation) was highest for PP3 (1097.31 kN·mm), closely followed by PP5 and PP7. This reinforces the conclusion that a moderate fiber content achieves the best overall flexural performance by balancing strength, ductility, and toughness.

These findings are in agreement with previous research on synthetic fiber-reinforced concrete. For example, Shi et al. (2020) reported that PP fibers in optimized dosages enhance both strength and post-cracking performance, while excessive volumes may reduce workability and uniformity. Similarly, Ding et al. (2020) highlighted that the fracture toughness of fiber-reinforced concrete is maximized at intermediate fiber dosages due to optimal crack-bridging efficiency.

From an engineering perspective, the results suggest that for applications prioritizing strength and toughness—such as bridge deck slabs or industrial floors—PP3 provides the most balanced performance. For seismic applications where ductility is critical, PP5 may be more advantageous. Conversely, where serviceability deflection control is the main concern, as in long-span beams, PP7's higher initial stiffness could be beneficial, provided the potential reduction in ductility is acceptable.

In summary, the flexural behavior results highlight the importance of dosage optimization in fiber-reinforced GGBFS concrete. Moderate fiber contents (3–5 kg/m^3) offer substantial improvements in load capacity, deformation ability, and toughness, whereas excessive fiber volumes may lead to marginal gains or even trade-offs in certain performance aspects due to workability challenges and stiffness–ductility interactions.

3.4 Crack Pattern Observation

The crack patterns observed at maximum load (P_{max}) and at ultimate load (P_{ult}) for all beam specimens are shown in Figure 4-7. Across all beams, the first visible cracks consistently appeared in the constant moment region between the two loading points, which is consistent with flexural behavior under four-point bending. However, the progression, distribution, and width of cracks varied significantly depending on the PP fiber content.

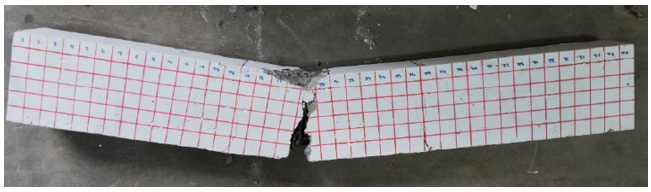

Figure 4 Crack pattern at peak load (P_{max}) for control beam (PP0) without fibers, showing single dominant mid-span crack indicating brittle failure.

For the control beam (PP0) shown in Figure 4, the first crack appeared at a relatively low load and propagated rapidly through the depth of the beam. Subsequent cracks developed sparsely and concentrated near mid-span, with limited branching. At P_{max}, one dominant crack became the primary failure path, widening significantly in the post-peak stage. This crack localization is characteristic of plain concrete beams, in which once the tensile capacity of the matrix is exceeded, stress transfer to reinforcement is immediate and concentrated, leading to rapid softening and brittle behavior.

In contrast, the fiber-reinforced beams exhibited more distributed and finer cracks. The PP3 beam developed multiple microcracks at lower load levels, but their growth rate slowed due to fiber bridging. At P_{max},

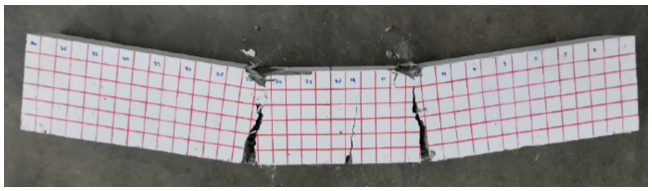

Figure 5 Crack pattern at peak load (P_{max}) for beam with 3 kg/m³ PP fibers (PP3), showing multiple fine cracks and reduced crack width due to effective crack bridging.

cracks remained narrower, and additional secondary cracks formed away from the main flexural zone, indicating improved stress redistribution. In the post-peak stage, the cracks continued to propagate gradually, with widths remaining within a moderate range due to the restraint provided by the fibers.

Figure 6 Crack pattern at ultimate failure load (P_{ult}) for beam with 5 kg/m³ PP fibers (PP5), exhibiting widely distributed narrow cracks consistent with highest ductility index.

The PP5 beam displayed an even denser network of cracks, extending over a wider portion of the span. The high crack density suggests that fibers effectively delayed the coalescence of microcracks into dominant cracks, which is beneficial for ductility. This finding aligns with the high ductility index recorded for PP5. The distribution of cracks also suggests a more uniform strain distribution along the tensile face of the beam, which is advantageous for seismic resistance because multiple yielding zones are preferred over a single plastic hinge formation.

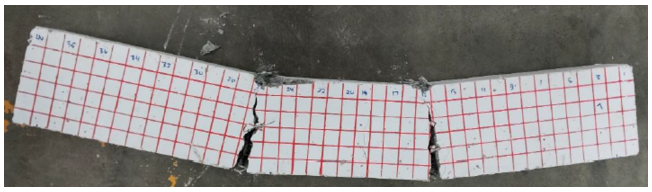

Figure 7 Crack at ultimate failure load (P_{ult}) for beam with 7 kg/m³ PP fibers (PP7), showing extensive distribution of fine cracks and gradual failure mode with high energy dissipation.

For the PP7 beam, although cracks were initially narrow, their density was lower than that in PP5. The increased stiffness of the high-fiber matrix limited deformation in the early stages, but once cracking initiated, several cracks propagated more abruptly. This behavior reflects a balance shift: while high fiber content restrains crack width effectively, it can also reduce the number of cracks by increasing the elastic stiffness, potentially limiting energy dissipation through microcracking.

A key observation across all fiber-reinforced beams is that crack widths at P_{ult} remained smaller than those in the control beam, even for the most heavily loaded cases. This improvement in crack control is directly related to the fiber-bridging mechanism, whereby PP fibers spanning across crack faces carry tensile forces after matrix cracking, reducing opening displacement. This mechanism is supported by microstructural studies (Ding et al., 2020; Shi et al., 2020), which show that PP fibers anchor into the surrounding paste, mobilizing pull-out resistance and friction along the fiber–matrix interface.

From a durability standpoint, improved crack control has significant implications. Narrower cracks limit the ingress of chlorides, sulfates, and other aggressive agents, enhancing the service life of structural elements in harsh environments, such as coastal infrastructure and bridge decks. In this context, the combination of GGBFS—known for its pore refinement and chloride binding capacity—with PP fibers offers a dual mechanism for durability enhancement: microstructural densification and mechanical crack restriction.

In summary, the crack pattern observations confirm the quantitative flexural performance results: moderate fiber dosages (3–5 kg/m³) promote distributed microcracking, higher ductility, and better energy dissipation, while excessive dosages (7 kg/m³) improve stiffness and crack width control but may reduce crack density and ductility. This nuanced understanding of crack behavior is essential for performance-based design, where serviceability, durability, and ultimate strength must be balanced for specific applications.

4 DISCUSSION

The experimental results provide a comprehensive understanding of the mechano-microstructural interaction between a dense GGBFS-based cementitious matrix and discrete PP fiber reinforcement in RC beams. The discussion in this section integrates compressive strength, flexural behavior, and crack pattern observations, offering insights into the mechanisms governing performance and their implications for structural concrete design.

4.1 Role of GGBFS in Matrix Densification and Strength Development

The compressive strength results confirmed that partial replacement of Portland cement with 30% GGBFS produced a dense and refined matrix that surpassed the strength of plain cement concrete beyond 28 days.

The microstructural densification was attributed to the pozzolanic and latent hydraulic reactions of GGBFS, which consume calcium hydroxide ($Ca(OH)_2$) and generate secondary C–S–H gel, reducing the porosity of the paste and improving the quality of the interfacial transition zone (ITZ). Studies on high-performance concrete have reported strength enhancement at 28 and 49 days with 30–50% GGBFS replacement (Yun et al., 2020). Similarly, microstructural investigations of blended systems with GGBFS and silica fume revealed reduced porosity, increased formation of C–S–H and C–A–S–H gels, and improved durability and compressive strength (Chen et al., 2024).

The replacement range of 30–40% GGBFS is frequently considered optimal, providing a favorable balance between later-age strength gain and early-age strength retention. Recent studies emphasize that mixtures within this range achieve the best trade-off between mechanical and durability performance (Ahmed, 2024; Dandaboina et al., 2025).

However, higher replacement levels, such as >40% GGBFS, may lead to lower long-term strength due to clinker dilution and insufficient $Ca(OH)_2$ for complete slag activation. This limitation has been confirmed in recent investigations, which observed increased porosity and reduced strength in mixes with very high SCM contents (Sadok et al., 2021; Dandaboina et al., 2025).

From a practical standpoint, the strength gain beyond 28 days is particularly advantageous for infrastructure subjected to sustained or gradually increasing service loads. In massive structural elements, the slower hydration of GGBFS can also mitigate thermal cracking by reducing peak hydration temperatures.

4.2 PP Fiber Contribution to Compressive Strength

The incorporation of PP fibers at 3 kg/m³ into the optimized 30% GGBFS matrix enhanced compressive strength by approximately 44% at 28 days and about 5% at 56 days compared to the fiber-free control. This improvement at a moderate fiber dosage can be explained by enhanced crack resistance under compression, where fibers bridge internal flaws and restrain microcrack propagation during loading.

However, increasing fiber dosage beyond 3 kg/m³ did not yield additional strength gains, and in some cases slightly reduced compressive strength. This reduction can be attributed to reduced workability and increased risk of fiber balling, leading to air void entrapment and localized paste discontinuities. These results align with (Mohamed and Zuaiter, 2024), who emphasized the importance of optimal fiber content to avoid negative effects on matrix homogeneity.

4.3 Flexural Behavior: Strength–Ductility–Toughness Interactions

The flexural test results reveal that PP fibers significantly modify the load–deflection response of RC beams. The 3 kg/m³ dosage (PP3) yielded the highest peak load (P_{max}), demonstrating improved cracking resistance and stress transfer prior to reinforcement yielding. The 5 kg/m³ dosage (PP5) provided the highest ductility index, indicating superior deformation capacity before failure, while the 7 kg/m³ dosage (PP7) maximized initial stiffness and post-peak energy dissipation.

The differences in performance can be linked to fiber–matrix interaction mechanisms. At moderate dosages, fibers are well-dispersed, enhancing crack-bridging efficiency and maintaining good workability. At higher dosages, despite increased stiffness and post-cracking resistance, the risk of non-uniform distribution and matrix discontinuities becomes more significant, reducing the efficiency of fiber reinforcement in the elastic range.

This finding is consistent with Jang et al. (2017), who reported that optimal fiber dosages enhance both flexural strength and ductility, whereas excessive fiber content can reduce these benefits due to workability challenges.

4.4 Crack Control and Durability Implications

Crack pattern observations demonstrated that PP fibers effectively transformed the fracture mode from brittle localization (in control beams) to distributed microcracking (in fiber-reinforced beams). The narrower crack widths in fiber-reinforced beams not only improved structural aesthetics and serviceability but also provided substantial durability benefits by reducing pathways for aggressive agents.

When combined with GGBFS's chloride-binding capability and reduced permeability, the fiber-induced crack control could significantly extend service life, particularly in marine and salt-exposed environments. These synergistic benefits are highly relevant to performance-based durability design, which is increasingly emphasized in modern infrastructure projects.

4.5 Trade-Offs and Performance-Based Design Guidance

The results highlight important trade-offs between stiffness, strength, ductility, and toughness. For example, while PP7 exhibited the highest stiffness, it also had the lowest ductility among fiber-reinforced beams. Conversely, PP5 achieved the highest ductility but a slightly lower peak load than PP3.

This finding underscores the importance of selecting the appropriate fiber dosage based on the specific performance priorities of the structure. For strength-dominated applications, such as heavily loaded beams or short-span girders, PP3 provides the most favorable balance between load capacity and structural efficiency. In cases where ductility is the primary requirement, as in seismic frame beams or plastic hinge zones, PP5 offers superior deformation capacity before failure. Meanwhile, for serviceability-critical structures, including long-span floor beams or deflection-sensitive members, PP7 delivers the highest stiffness and effective control of crack widths, thereby enhancing overall service performance. Such selections align with the concept of performance-based design, where material composition is optimized to meet project-specific serviceability, safety, and durability targets rather than pursuing a single "maximum" property value.

4.6 Limitations and Future Research Directions

While the study provides valuable insights, several limitations should be acknowledged. First, the testing program was limited to 56 days; extended testing to 90 days or beyond would provide a more complete understanding of long-term strength and durability performance, particularly given the continued hydration potential of GGBFS. Second, microstructural analysis (e.g., SEM, EDS) was not conducted within this experimental phase but would offer direct evidence of fiber–matrix bonding and pore refinement mechanisms. Finally, field-scale validation is necessary to confirm laboratory results under real placement, compaction, and curing conditions.

Future research should also explore hybrid fiber systems, where PP fibers are combined with steel or basalt fibers, potentially enhancing both tensile and compressive properties while improving post-cracking behavior. Additionally, the influence of fiber geometry (length, aspect ratio, and surface texture) on GGBFS-based concrete performance warrants further investigation.

5 CONCLUSION

This study investigated the combined effects of GGBFS and PP fibers on the mechanical behavior of reinforced concrete beams, with particular emphasis on compressive strength, flexural response, and crack development. Experimental findings revealed that replacing 30% of Portland cement with GGBFS produced the highest later-age compressive strength, surpassing the control mix at both 28 and 56 days. This enhancement is attributed to microstructural densification through secondary C–S–H formation, which is consistent with the widely reported optimal GGBFS replacement range of 30–45%.

The incorporation of PP fibers further contributed to strength and flexural performance improvements. A moderate dosage of 3 kg/m^3 provided the greatest gain in compressive strength, with increases of up to 44% at 28 days, whereas higher dosages (5–7 kg/m^3) yielded no additional benefits due to reduced workability and fiber clustering. Flexural tests demonstrated superior performance across all fiber-reinforced beams compared to the control. Specifically, the PP3 mixture achieved the highest peak load capacity, PP5 provided the greatest ductility index, and PP7 offered superior initial stiffness and post-peak energy dissipation.

Beyond mechanical performance, PP fibers effectively transformed brittle crack localization into distributed microcracking, significantly limiting crack widths at ultimate load. Coupled with the reduced permeability and chloride-binding capacity imparted by GGBFS, this synergy enhances durability and service life in aggressive environments. These findings highlight the importance of tailoring fiber dosage to design priorities: PP3 for strength-critical applications, PP5 for ductility-driven performance, and PP7 for serviceability and crack control.

Overall, the integration of 30% GGBFS with optimally dosed PP fibers demonstrates a viable pathway toward sustainable and high-performance structural concrete. The observed synergy improves mechanical behavior, crack control, and long-term durability in ways that are aligned with modern performance-based design frameworks. Future work should include extended curing studies, detailed microstructural characterization, and full-scale field trials to validate these results and refine practical design guidelines.

DISCLAIMER

The authors declare no conflict of interest regarding the funding, authorship, or publication of this research.

ACKNOWLEDGMENTS

The authors would like to express their gratitude to PT Krakatau Semen Indonesia for providing the GGBFS material used in this research. The authors also acknowledge PT Global Pro Asia, the country distributor of Kratos in Indonesia, for supplying the polypropylene fibers.

REFERENCES

Ahmad, J., Burduhos-Nergis, D. D., Arbili, M. M., Alogla, S. M., Majdi, A. and Deifalla, A. F. (2022), 'A review on failure modes and cracking behaviors of polypropylene fibers reinforced concrete', *Buildings* .
URL: *https://doi.org/10.3390/buildings12111951*

Ahmed, A. (2024), 'Assessing the effects of supplementary cementitious materials on concrete properties: A review', *Discover Civil Engineering* .
URL: *https://doi.org/10.1007/s44290-024-00154-z*

Banthia, N. and Gupta, R. (2006), 'Influence of polypropylene fiber geometry on plastic shrinkage cracking in concrete', *Cement and Concrete Research* .
URL: *https://doi.org/10.1016/j.cemconres.2006.01.010*

Bertelsen, I., Ottosen, L. and Fischer, G. (2020), 'Influence of fibre characteristics on plastic shrinkage cracking in cement-based materials: A review', *Construction and Building Materials* .
URL: *https://doi.org/10.1016/j.conbuildmat.2019.116769*

Bhogone, M. V. and Subramaniam, K. V. L. (2021), 'Early-age tensile constitutive relationships for steel and polypropylene fiber reinforced concrete', *Engineering Fracture Mechanics* .
URL: *https://doi.org/10.1016/j.engfracmech.2021.107556*

Chen, W., Wu, M. and Liang, Y. (2024), 'Effect of sf and ggbs on pore structure and transport properties of concrete', *Materials* **17**(6).
URL: *https://doi.org/10.3390/ma17061365*

Dandaboina, K., Prasad, J. S. and Sohail, S. (2025), 'Mechanical and microstructural properties of concrete with partial replacement of fine aggregate by steel slag and cement by ggbfs and metakaolin', *Discover Civil Engineering* **2**(1).
URL: *https://doi.org/10.1007/s44290-025-00180-5*

Ding, Y., Zeng, W., Wang, Q. and Zhang, Y. (2020), 'Topographical analysis of fractured surface roughness of macro fiber reinforced concrete and its correlation with flexural toughness', *Construction and Building Materials* .
URL: *https://doi.org/10.1016/j.conbuildmat.2019.117466*

Ebead, U., Shrestha, K. C., Afzal, M. S., El Refai, A. and Nanni, A. (2017), 'Effectiveness of fabric-reinforced cementitious matrix in strengthening reinforced concrete beams', *Journal of Composites for Construction* .
URL: *https://doi.org/10.1061/(ASCE)CC.1943-5614.0000741*

El Mennaouy, F., Ouadia, M., Bybi, A., Khanfri, C. and Nakach, I. (2025), 'Impact of corrosion on the bonding properties at the concrete-rebar interface in reinforced concrete structures', *Results in Engineering* **26**, 105615.
URL: *https://doi.org/10.1016/J.RINENG.2025.105615*

Gali, S. and Subramaniam, K. V. L. (2019), 'Cohesive stress transfer and shear capacity enhancements in hybrid steel and macro-polypropylene fiber reinforced concrete', *Theoretical and Applied Fracture Mechanics* .
URL: *https://doi.org/10.1016/j.tafmec.2019.102250*

Guo, H., Jiang, L., Tao, J., Chen, Y., Zheng, Z. and Jia, B. (2021), 'Influence of a hybrid combination of steel and polypropylene fibers on concrete toughness', *Construction and Building Materials* .
URL: *https://doi.org/10.1016/j.conbuildmat.2020.122132*

Hatami Jorbat, M., Hosseini, M. and Mahdikhani, M. (2020), 'Effect of polypropylene fibers on the mode i, mode ii, and mixed-mode fracture toughness and crack propagation in fiber-reinforced concrete', *Theoretical and Applied Fracture Mechanics* .
URL: *https://doi.org/10.1016/j.tafmec.2020.102723*

Hawileh, R. A., Abdalla, J. A., Fardmanesh, F., Shahsana, P. and Khalili, A. (2017), 'Performance of reinforced concrete beams cast with different percentages of ggbs replacement to cement', *Archives of Civil and Mechanical Engineering* .
URL: *https://doi.org/10.1016/j.acme.2016.11.006*

Helmi, M. and Alraimi, A. (2024), 'Effects of carbon fiber on mechanical properties of reactive powder concrete', *Journal of the Civil Engineering Forum* **10**(3), 239–248.
URL: *https://doi.org/10.22146/jcef.12439*

Hendra, M., Putri, S. and Herdianto, M. (2025), 'Compressive and flexural properties of the kevlar fiber as a textile-reinforced concrete for lightweight construction applications', *Journal of the Civil Engineering Forum* **11**(3), 341–352.
URL: *https://doi.org/10.22146/jcef.18303*

Hossain, M., Islam, G. and Mallick, A. (2022), 'Compressive strength prediction for industrial waste-based scc using artificial neural network', *Journal of the Civil Engineering Forum* **9**(1), 11–26.
URL: *https://doi.org/10.22146/jcef.4094*

Hussain, F., Kaur, I. and Hussain, A. (2020), 'Reviewing the influence of ggbfs on concrete properties', *Materials Today: Proceedings* .
URL: *https://doi.org/10.1016/j.matpr.2020.07.410*

Imran, H., Ibrahim, M., Al-Shoukry, S., Rustam, F. and Ashraf, I. (2022), 'Latest concrete materials dataset and ensemble prediction model for concrete compressive strength containing rca and ggbfs materials', *Construction and Building Materials* .
URL: *https://doi.org/10.1016/j.conbuildmat.2022.126525*

Jang, S. Y., Karthick, S. and Kwon, S. J. (2017), 'Investigation on durability performance in early aged high-performance concrete containing ggbfs and fa', *Advances in Materials Science and Engineering* .
URL: *https://doi.org/10.1155/2017/3214696*

Khan, M., Cao, M., Xie, C. and Ali, M. (2022), 'Effectiveness of hybrid steel-basalt fiber reinforced concrete under compression', *Case Studies in Construction Materials* .
URL: *https://doi.org/10.1016/j.cscm.2022.e00941*

Lakshmi, A., Pandit, P., Bhagwat, Y. and Nayak, G. (2022), A review on efficiency of polypropylene fiber-reinforced concrete, *in* 'Lecture Notes in Civil Engineering'.
URL: *https://doi.org/10.1007/978-981-16-2826-9_50*

Li, B., Chi, Y., Xu, L., Shi, Y. and Li, C. (2018), 'Experimental investigation on the flexural behavior of steel-polypropylene hybrid fiber reinforced concrete', *Construction and Building Materials* .
URL: *https://doi.org/10.1016/j.conbuildmat.2018.09.202*

Li, G., Zhang, A., Song, Z., Liu, S. and Zhang, J. (2018), 'Ground granulated blast furnace slag effect on the durability of ternary cementitious system exposed to combined attack of chloride and sulfate', *Construction and Building Materials* .
URL: *https://doi.org/10.1016/j.conbuildmat.2017.10.062*

Li, J. J., Niu, J. G., Wan, C. J., Jin, B. and Yin, Y. L. (2016), 'Investigation on mechanical properties and microstructure of high performance polypropylene fiber reinforced lightweight aggregate concrete', *Construction and Building Materials* .
URL: *https://doi.org/10.1016/j.conbuildmat.2016.04.116*

Liang, N., Ren, L., Tian, S., Liu, X., Zhong, Z., Deng, Z. and Yan, R. (2021), 'Study on the fracture toughness of polypropylene–basalt fiber-reinforced concrete', *International Journal of Concrete Structures and Materials* .
URL: *https://doi.org/10.1186/s40069-021-00472-x*

Ling, J., Lim, Y. and Jusli, E. (2023), 'Methods to determine ductility of structural members: A review', *Journal of the Civil Engineering Forum* **9**(2), 181–194.
URL: *https://doi.org/10.22146/jcef.6631*

Liu, Y., Wang, L., Cao, K. and Sun, L. (2021), 'Review on the durability of polypropylene fibre-reinforced concrete', *Advances in Civil Engineering* .
URL: *https://doi.org/10.1155/2021/6652077*

Majhi, R. K. and Nayak, A. N. (2019), 'Bond, durability and microstructural characteristics of ground granulated blast furnace slag based recycled aggregate concrete', *Construction and Building Materials* .
URL: *https://doi.org/10.1016/j.conbuildmat.2019.04.017*

Michalik, A., Chyliński, F., Bobrowicz, J. and Pichór, W. (2022), 'Effectiveness of concrete reinforcement with recycled tyre steel fibres', *Materials* .
URL: *https://doi.org/10.3390/ma15072444*

Mohamed, O. and Zuaiter, H. (2024), 'Fresh properties, strength, and durability of fiber-reinforced geopolymer and conventional concrete: A review', *Polymers* .
URL: *https://doi.org/10.3390/polym16010141*

Muralidharan, R., Park, T., Yang, H., Lee, S., Subbiah, K. and Lee, H. (2021), 'Review of the effects of supplementary cementitious materials and chemical additives on the physical, mechanical and durability properties of hydraulic concrete', *Materials* .
URL: *https://doi.org/10.3390/ma14237270*

Oner, A. and Akyuz, S. (2007), 'An experimental study on optimum usage of ggbs for the compressive strength of concrete', *Cement and Concrete Composites* .
URL: *https://doi.org/10.1016/j.cemconcomp.2007.01.001*

Prasanna, P. K., Srinivasu, K. and Ramachandra Murthy, A. (2021), Strength and durability of fiber reinforced concrete with partial replacement of cement by ground granulated blast furnace slag, *in* 'Materials Today: Proceedings'.
URL: *https://doi.org/10.1016/j.matpr.2021.06.267*

Qin, F., Zhang, Z., Yin, Z., Di, J., Xu, L. and Xu, X. (2020), 'Use of high strength, high ductility engineered cementitious composites (ecc) to enhance the flexural performance of reinforced concrete beams', *Journal of Building Engineering* .
URL: *https://doi.org/10.1016/j.jobe.2020.101746*

Qin, Y., Zhang, X., Chai, J., Xu, Z. and Li, S. (2019), 'Experimental study of compressive behavior of polypropylene-fiber-reinforced and polypropylene-fiber-fabric-reinforced concrete', *Construction and Building Materials* .
URL: *https://doi.org/10.1016/j.conbuildmat.2018.11.042*

Ríos, J., Cifuentes, H., Leiva, C., Ariza, M. and Ortiz, M. (2020), 'Effect of polypropylene fibers on the fracture behavior of heated ultra-high performance concrete', *International Journal of Fracture* .
URL: *https://doi.org/10.1007/s10704-019-00407-4*

Sadok, R., Maherzi, W., Benzerzour, M., Lord, R., Torrance, K., Zambon, A. and Abriak, N. (2021), 'Mechanical properties and microstructure of low carbon binders manufactured from calcined canal sediments and ground granulated blast furnace slag (ggbs)', *Sustainability (Switzerland)* .
URL: *https://doi.org/10.3390/su13169057*

Shao, Y., Nguyen, W., Bandelt, M., Ostertag, C. and Billington, S. (2022), 'Seismic performance of high-performance fiber-reinforced cement-based composite structural members: A review', *Journal of Structural Engineering* .
URL: *https://doi.org/10.1061/(asce)st.1943-541x.0003428*

Shi, F., Pham, T., Hao, H. and Hao, Y. (2020), 'Post-cracking behaviour of basalt and macro polypropylene hybrid fibre reinforced concrete with different compressive strengths', *Construction and Building Materials* .
URL: *https://doi.org/10.1016/j.conbuildmat.2020.120108*

Syll, A. and Kanakubo, T. (2022), 'Impact of corrosion on the bond strength between concrete and rebar: A systematic review', *Materials* .
URL: *https://doi.org/10.3390/ma15197016*

Turker, K. and Torun, I. (2020), 'Flexural performance of highly reinforced composite beams with ultra-high performance fiber reinforced concrete layer', *Engineering Structures* .
URL: *https://doi.org/10.1016/j.engstruct.2020.110722*

Xiong, X., Yang, Z., Yan, X., Zhang, Y., Dong, S., Li, K., Briseghella, B. and Marano, G. (2023), 'Mechanical properties and microstructure of engineered cementitious composites with high volume steel slag and ggbfs', *Construction and Building Materials* **398**, 132512.
URL: *https://doi.org/10.1016/J.CONBUILDMAT.2023.132512*

Yan, S., Dong, Q., Chen, X., Li, J., Wang, X. and Shi, B. (2024), 'An experimental and numerical study on the hybrid effect of basalt fiber and polypropylene fiber on the impact toughness of fiber reinforced concrete', *Construction and Building Materials* .
URL: *https://doi.org/10.1016/j.conbuildmat.2023.134270*

Yun, C., Rahman, M., Phing, C., Chie, A. and Bakri, M. B. (2020), 'The curing times effect on the strength of ground granulated blast furnace slag (ggbfs) mortar', *Construction and Building Materials* .
URL: *https://doi.org/10.1016/j.conbuildmat.2020.120622*

Özbay, E., Erdemir, M. and Durmuş, H. I. (2016), 'Utilization and efficiency of ground granulated blast furnace slag on concrete properties – a review', *Construction and Building Materials* .
URL: *https://doi.org/10.1016/j.conbuildmat.2015.12.153*